Engineering Structures 124 (2016) 245–257

Contents lists available at ScienceDirect

Engineering Structures

journal homepage: www.elsevier.com/locate/engstruct

Influence of adjusted models of plastic hinges in nonlinear behaviour of reinforced concrete buildings

Andrés López-López, Antonio Tomás *, Gregorio Sánchez-Olivares

Department of Civil Engineering, Universidad Politécnica de Cartagena (UPCT), Paseo Alfonso XIII, 52, 30203 Cartagena, Spain

ARTICLE INFO

Article history:
Received 3 June 2015
Revised 11 June 2016
Accepted 13 June 2016
Available online 29 June 2016

Keywords:
Reinforced concrete
Yield/ultimate behaviour
Plastic hinge
Nonlinear analysis

ABSTRACT

Among the procedures available for the seismic analysis of structures, pushover analysis is one of the most frequently used methods by structural engineers. An adequate modelling of the plastic hinges generated during the pushover analysis is crucial in order to obtain accurate results. Thus, the yielding and ultimate states of the cross-section must be defined in order to model the generalised force-deformation relation of plastic hinges. For this purpose, the use of empirical expressions that obtain the aforementioned states from the cross-section properties can prove beneficial.

The main objective of this work is to study the influence of different plastic hinge models on the structural nonlinear behaviour of reinforced concrete structures. To that end, several nonlinear analyses have been performed with the software SAP2000®, considering the following plastic hinge models: (i) the model of FEMA-356 included in SAP2000®, and (ii) two additional models developed by some researchers by using empirical expressions calibrated with different experimental data. Simplified structures of two buildings have been used as examples.

The results obtained show that plastic hinges modelled with empirical expressions can be used by structural engineers to more precisely model the behaviour of structural elements in ordinary reinforced concrete buildings located in seismic areas, and to compare with the results offered by the models included in seismic building design codes.

1. Introduction

The prediction and simulation of the seismic behaviour of structures by using numerical models has been a field of growing interest in recent years, due to the importance of accurately knowing the effects and consequences caused by seismic actions on structures.

Seismic analysis can be performed by following different procedures, with differing degrees of accuracy achieved in the results. Nonlinear static analysis or pushover is one of the most frequently employed methods by structural engineers, due to its relative simplicity and the guidelines offered by the main seismic building design codes for its implementation. This analysis offers relevant information from the seismic point of view, such as the resistance and the deformation capacity of the structure. Pushover analysis can be implemented through different strategies, such as the modal pushover [1], the consecutive modal pushover [2], the upper bound pushover [3], the mass proportional pushover [4] and the adaptive pushover [5]. However, the increase in accuracy of all these methods is at the expense of the most attractive feature of conventional pushover analysis, namely its simplicity [6]. Therefore, conventional pushover analyses [7] have been implemented in the current study.

Adequate knowledge of the sectional behaviour of structural elements at yield and ultimate states is necessary in order to define the properties of the plastic hinges generated in the structure during nonlinear analysis. Thus, the yield moment M_y, the yield chord rotation θ_y and the ultimate chord rotation θ_u of the element's section are used to model the moment-chord rotation relations that define the behaviour of plastic hinges during the analysis.

In the seismic analysis of structures, the use of empirical expressions that reproduce the yield and ultimate states of a structural element's section is beneficial [8–10]. These expressions are accurate and efficient from the point of view of computation time, due to their relative simplicity and the fact that they are calibrated with experimental tests.

The main objective of the present work is the evaluation of the influence of the type of plastic hinge considered in the nonlinear behaviour of structures. To do so, several pushover analyses have

* Corresponding author.
E-mail addresses: atll0@alu.upct.es (A. López-López), antonio.tomas@upct.es (A. Tomás), gregorio.sanchez@upct.es (G. Sánchez-Olivares).

http://dx.doi.org/10.1016/j.engstruct.2016.06.021
0141-0296/

Notation

a	confinement effectiveness factor
a_{cy}	zero-one variable for the type of loading (0 for monotonic loading, 1 for cyclic loading)
a_g	design ground acceleration on type A ground, defined in EC-8
a_{sl}	zero-one variable for slip (0 if slip of longitudinal bars from the anchorage is not physically possible, 1 if it is)
a_{st}	coefficient for the type of steel (0.0185 for hot-rolled or heat-treated steel, 0.0115 for cold-worked steel)
a_v	zero-one variable for diagonal cracking before flexural yielding of the end section
$a_{w,r}$	zero-one variable for rectangular walls (1 for rectangular walls, 0 for beams and columns)
$a_{w,nr}$	zero-one variable for non-rectangular sections (1 for T-, H-, U- or hollow rectangular sections; 0 for rectangular sections)
A_{sh}	area of lateral reinforcement
b	width of rectangular cross-section
d	distance from extreme compression fibre to centroid of tension reinforcement
d'	distance from extreme compression fibre to centroid of compression reinforcement
d_t	target displacement of the structure
E_c	modulus of elasticity of concrete
E_s	modulus of elasticity of reinforcement
f_c	compressive strength of unconfined concrete based on standard cylinder test
f_y	yield strength of tension reinforcement
f_y'	yield strength of compression reinforcement
f_{yh}	yield strength of lateral reinforcement
f_{yv}	yield strength of web longitudinal reinforcement
F_b	seismic base shear force
F_i	lateral force applied in the i-storey
g	acceleration of gravity
$G_{k,j}$	characteristic permanent action
h	height of rectangular cross-section
h_i	height from the base to i-storey
h_j	height from the base to j-storey
k	parameter with values depending on the fundamental mode T
L_s	shear span of member (= M/V at the end of the member)
m_i	mass of the i-storey
m_j	mass of the j-storey
M	bending moment
M_y	yield moment
N	axial force
$Q_{k,i}$	characteristic variable action
s_h	spacing of lateral reinforcement
s_i	displacement of the mass m_i in the fundamental mode shape
S_a	spectral acceleration
S_d	spectral displacement
V	shear force
z	internal lever arm
δ	control displacement, located at the centre of mass of the top storey of the structure
δ'	$=d'/d$
θ_y	yield chord rotation
θ_u	ultimate chord rotation
ν	normalised axial load, N/bhf_c
ξ_y	neutral axis depth at yielding, normalised to d
$\psi_{E,i}$	combination coefficient for a variable action i, to be used when determining the effects of the design seismic action
ρ	tension reinforcement ratio, determined as ratio of tension reinforcement area to bd
ρ'	compression reinforcement ratio, determined as ratio of compression reinforcement area to bd
ρ_d	diagonal reinforcement ratio in diagonally reinforced members, determined as ratio of area of reinforcement arranged along one diagonal to bd
ρ_h	lateral reinforcement ratio (= A_{sh}/bs_h)
ρ_v	ratio of web longitudinal reinforcement, uniformly distributed between tension and compression reinforcement, normalised to bd
ϕ_L	diameter of tension reinforcement bars
ϕ_y	yield curvature of the cross-section
ω_1	total mechanical reinforcement ratio of tension and web longitudinal bars [= $(\rho f_y + \rho_v f_{yv})/f_c$]
ω_2	mechanical reinforcement ratio of compression reinforcement [= $\rho' f_y'/f_c$]

been implemented in two reinforced concrete structures, considering the following types of plastic hinges:

(i) Plastic hinges modelled from FEMA-356 [11], included by default in the software SAP2000® [12],
(ii) plastic hinges defined with the empirical expressions available in [9,10], and
(iii) plastic hinges modelled with the expressions developed by the authors [13,14].

In order to define the properties of the plastic hinges considered, the moment-chord rotation relations of the sections are obtained with the aforementioned methods. With the aim of considering the influence of the axial force N in the value of the yield moment M_y, some yielding curves N-M_y are defined for the columns of the structures.

In pushover analysis, it is important to study the global yielding and collapse points of the structure, which offer information about the ductility. Thus, the control displacement δ, the seismic base shear force F_b and the spectral acceleration S_a corresponding to those points are obtained. Additionally, the capacity curves F_b - δ of the structures are obtained.

Finally, the N2 method [15] proposed in EC-8 is implemented for two structures. Some ground acceleration values a_g are considered in order to study the influence of this parameter in the differences obtained with the different types of plastic hinges. Nonlinear time history analyses are performed to contrast with the results obtained using pushover analyses.

2. Plastic hinges models and analysis methodology

2.1. Equations for the sectional behaviour

Several expressions are suitable to reproduce the yielding and ultimate states of reinforced concrete sections from their geometry, reinforcement distribution and the mechanical properties of materials. In this line, Panagiotakos and Fardis [8] proposed several expressions to obtain the yield moment M_y, the yield chord rotation θ_y and the ultimate chord rotation θ_u. These expressions were calibrated with a database of more than 1000 experimental tests corresponding to beams, columns and shear walls. Later, Biskinis and Fardis [9,10] modified these expressions by calibrating them using an experimental database that included retrofitted elements.

Finally, EC-8 [16] provides several equations to obtain the yield and ultimate chord rotation of sections.

The expressions proposed by Biskinis and Fardis [9,10] correspond to Eqs. (1)–(3).

$$\frac{M_y}{bd^3}=\phi_y\left\{E_c\frac{\xi_y^2}{2}\left(\frac{1+\delta'}{2}-\frac{\xi_y}{3}\right)+\frac{E_s(1-\delta')}{2}\left[(1-\xi_y)\rho+(\xi_y-\delta')\rho'+\frac{\rho_v}{6}(1-\delta')\right]\right\} \tag{1}$$

$$\theta_y=\phi_y\frac{L_s+a_v z}{3}+0.0014\left(1+1.5\frac{h}{L_s}\right)+a_{sl}\frac{\phi_y\phi_L f_y}{8\sqrt{f_c}} \tag{2}$$

$$\theta_u=a_{st}(1-0.43a_{cy})\left(1+\frac{a_{sl}}{2}\right)(1-0.42a_{w,r})\left(1-\frac{2}{7}a_{w,nr}\right)(0.3^{\nu})\times\left[\frac{\max(0.01;\omega_2)}{\max(0.01;\omega_1)}f_c\right]^{0.225}\left[\min\left(9,\frac{L_s}{h}\right)\right]^{0.35}25^{[(a\rho_h f_{yh})/f_c]}1.25^{100\rho_d} \tag{3}$$

The authors of the present work proposed other expressions to obtain M_y, θ_y and θ_u [13,14]. For this purpose, the expressions of Biskinis and Fardis [9,10] were calibrated with a selection of tests composed by reinforced concrete beams and columns with rectangular section, obtained from an experimental database of more than 1000 tests included in [8]. To obtain the aforementioned selection of tests, the seismic and constructional prescriptions included in the main design codes were imposed over the initial database. Specifically, the codes EC-2 [17], EC-8 [18] and ACI-318 [19] were considered.

Since the variables involved in the specimens in [8] presented such a wide range of values, five groups of parameters were chosen to meet the constructional requirements imposed by the building codes considered, which also implies considering a certain ductility level. The groups chosen were: the dimensions of the cross section; mechanical properties of materials; diameter of reinforcement bars; area of reinforcement steel; and spacing of lateral reinforcement. As some of these parameters (dimensions of cross section, area of reinforcement steel and spacing of lateral reinforcement) are directly related to the level of ductility to consider, the widest possible range of their values has been chosen so that, fulfilling the requirements of seismic codes leads to considering only real elements (designed and built under a certain seismic code) and covering a wide range of ductility behaviour.

New coefficients (C_1 to C_{15}) for the expressions in [9,10] were proposed for the calibration with the empirical results from the test selection. It is worth mentioning that, despite the theoretical basis of the expressions in [9,10], they also include several empirical coefficients obtained from the calibration with a database of experimental tests. The new coefficients C_i were proposed by performing a sensitivity analysis on the terms of the expressions in [9,10], which led to modifying mainly their empirical coefficients.

The expressions affected by the new coefficients are given by Eqs. (4)–(6):

$$\frac{M_y}{bd^3}=\phi_y\left\{E_c\frac{\xi_y^2}{2}\left(C_1\frac{1+\delta'}{2}-C_2\frac{\xi_y}{3}\right)+\frac{E_s(1-\delta')}{2}\times\left[C_3(1-\xi_y)\rho+C_4(\xi_y-\delta')\rho'+C_5\frac{\rho_v}{6}(1-\delta')\right]\right\} \tag{4}$$

$$\theta_y=\phi_y\frac{C_6L_s+C_7a_v z}{3}+C_8\left(1+C_9\frac{h}{L_s}\right)+C_{10}a_{sl}\frac{\phi_y\phi_L f_y}{8\sqrt{f_c}} \tag{5}$$

$$\theta_u=a_{st}(1-C_{11}a_{cy})\left(1+\frac{a_{sl}}{2}\right)(1-0.42a_{w,r})\left(1-\frac{2}{7}a_{w,nr}\right)(C_{12}^{\nu})\times\left[\frac{\max(0.01;\omega_2)}{\max(0.01;\omega_1)}f_c\right]^{C_{13}}\left[\min\left(9,\frac{L_s}{h}\right)\right]^{C_{14}}25^{[(a\rho_h f_{yh})/f_c]}C_{15}^{100\rho_d} \tag{6}$$

To achieve the best calibration of the expressions with the selection of tests, an optimization procedure based on Genetic Algorithms (GA) was implemented. The variables of the optimization problem are the coefficients from C_1 to C_{15}. The objective function to be minimized is the variation coefficient C_v of a variable x defined as the ratio of the experimental value x_{exp} and the predicted value x_{pred} (obtained from the expressions affected by the coefficients C_1 to C_{15}) for each test of the selection. Several statistical parameters of the variable $x = x_{exp}/x_{pred}$ were obtained, such as the aforementioned variation coefficient C_v, the sample mean $\bar{x}$, the sample standard deviation s and the sample linear correlation coefficient r between experimental and predicted values. Moreover, the summation S_d of the absolute values of the differences between experimental and predicted values was used to provide an estimate of the quality of the results (the more the summation reduces, the more accurate the calibration model is):

$$S_d=\sum_{i=1}^{m}|x_{i,\mathrm{exp}}-x_{i,\mathrm{pred}}| \tag{7}$$

The expressions obtained after running the GA procedure are presented in Eqs. (8)–(10).

$$\frac{M_y}{bd^3}=\phi_y\left\{\begin{array}{l}E_c\frac{\xi_y^2}{2}\left(1.40\frac{1+\delta'}{2}-1.90\frac{\xi_y}{3}\right)+\frac{E_s(1-\delta')}{2}[1.50(1-\xi_y)\rho\\+0.10(\xi_y-\delta')\rho'+0.10\frac{\rho_v}{6}(1-\delta')]\end{array}\right\} \tag{8}$$

$$\theta_y=\phi_y\frac{1.594L_s+2.552a_v z}{3}-0.0031\left(1-1.741\frac{h}{L_s}\right)+1.270a_{sl}\frac{\phi_y\phi_L f_y}{8\sqrt{f_c}} \tag{9}$$

$$\theta_u=a_{st}(1-0.167a_{cy})\left(1+\frac{a_{sl}}{2}\right)(1-0.42a_{w,r})\left(1-\frac{2}{7}a_{w,nr}\right)(0.237^{\nu})\times\left[\frac{\max(0.01;\omega_2)}{\max(0.01;\omega_1)}f_c\right]^{0.093}\left[\min\left(9,\frac{L_s}{h}\right)\right]^{0.537}25^{[(a\rho_h f_{yh})/f_c]}1.004^{100\rho_d} \tag{10}$$

It should be mentioned that the effects of shear influence the value obtained for θ_y. These effects are considered by the parameter a_v in Eq. (9). Thus, a_v equals 1 if flexural yielding is preceded by diagonal cracking, i.e., if the shear resistance of members without shear reinforcement V_{Rc} is less than the shear force at yielding of the end section M_y/L_s. If this is not the so, then the parameter a_v equals 0. Moreover, the second term of Eq. (9) is attributed to shear deformations along L_s.

A summary of the improvement ranges achieved in some statistical parameters when applying the expressions proposed in [13] with respect to other expressions is shown in Table 1. The expressions developed in [13] reduce the scatter (lower values of s, CV and S_d) and improve the linear relation between predicted and experimental values, with higher values being obtained for the correlation coefficient r.

The main contribution of the expressions developed in [13] is not the improvement achieved with respect to the previous equations, but the fact that they are suitable for structural elements of ordinary reinforced concrete buildings located in seismic areas due to their calibration with the selection of tests. For more detailed information about Eqs. (8)–(10), see Refs. [13,14].

Table 1
Ranges of improvement achieved with the expressions proposed in [13] with respect to other expressions (in %).

	s	C_v	r	S_d
Panagiotakos and Fardis [8]	24–28	14–16	1–62	13–36
EC-8 [16]	18–19	10	25–29	16–20
Biskinis and Fardis [9,10]	14–28	3–16	1–16	9–19

2.2. Pushover analysis. Specific considerations

Several conventional pushover analyses considering an invariant lateral load pattern are performed in this work. Two vertical distributions of lateral loads have been considered in the analysis following the EC-8 guidelines: (i) a uniform pattern, based on lateral forces that are proportional to mass regardless of elevation, and (ii) a modal pattern, proportional to the displacement of masses in the fundamental mode shape. The two vertical distributions are obtained by applying Eqs. (11) and (12), respectively. In case the effect of higher modes is important in estimating the seismic response of the structure, Mortezaei and Ronagh [20] adopted the modal pattern given by Eq. (13), included in FEMA-356 [11].

$$F_i = \frac{m_i}{\sum m_i} F_b \tag{11}$$

$$F_i = F_b \frac{s_i m_i}{\Sigma s_i m_i} \tag{12}$$

$$F_i = F_b \frac{m_i h_i^k}{\sum_{j=1}^{n} m_j h_j^k} \tag{13}$$

Gravity loads are uniformly distributed on beams according to Eq. (14), included in EC-8 [18].

$$\Sigma G_{k,j} + \Sigma \psi_{E,i} Q_{k,i} \tag{14}$$

The analyses have been performed with SAP2000® [12], considering lumped plastic hinges with null length. The location of the plastic hinges needs to be defined by the user. In this study, the generated plastic hinges are only located at the end of the beams and columns.

The RC (reinforced concrete) plastic hinges considered in this study are modelled with moment-chord rotation relations defined through deformation control. These relations depend on the type of plastic hinge considered in the analysis. Thus, the plastic hinges included in SAP2000® by default exhibit the relation shown in Fig. 1, defined in FEMA-356 [11], whereas the plastic hinges defined with the expressions of [9,10,13] are modelled with the moment-chord rotation relations included in Fig. 2.

As stated in EC-8 [18], P-Delta effects are considered in pushover analysis and the flexural and shear stiffness properties of members are equal to one-half of the corresponding stiffness of the uncracked elements, in order to consider the effect of cracking.

FEMA-356 [11] defines three structural performance levels, namely Immediate Occupancy IO, Life Safety LS and Collapse Prevention CP. In this work, these levels correspond to 40%, 80% and 100% of the ultimate chord rotation θ_u for beams and 25%, 75% and 100% for columns. These values are similar to those considered by other authors [21]. Fig. 3 shows the structural performance levels in the force-deformation relation of a plastic hinge.

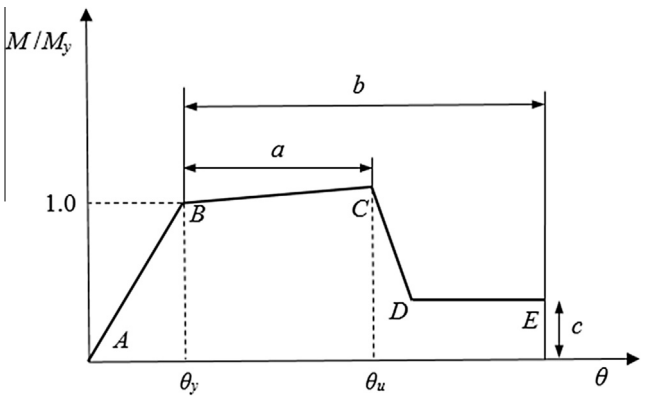

Fig. 1. Moment-chord rotation relation for RC plastic hinges [11].

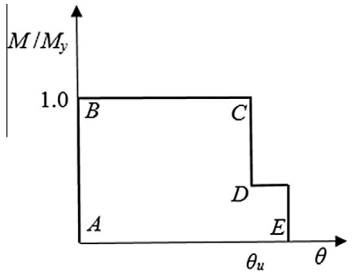

Fig. 2. Moment-chord rotation relation for RC plastic hinges [9,10,13].

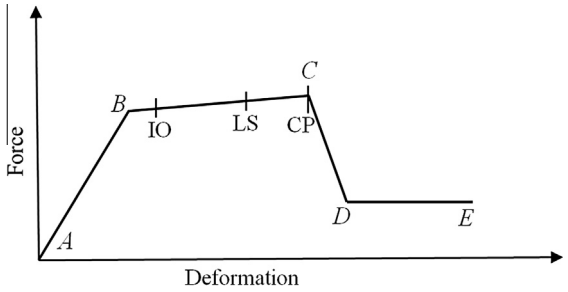

Fig. 3. Performance levels in plastic hinges.

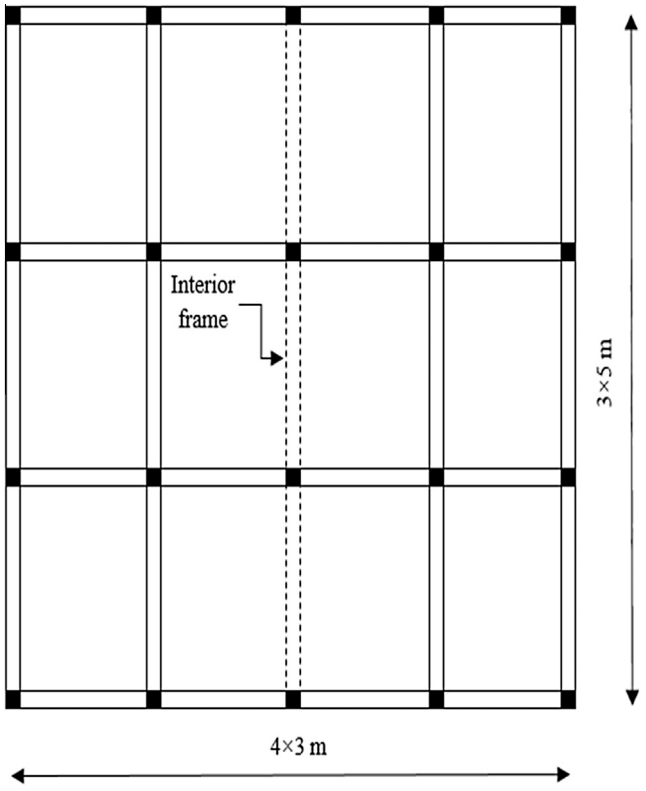

Fig. 4. Floor plan of usual 5- and 8-storey reinforced concrete buildings.

2.3. Influence of the ground acceleration a_g

The seismic response of a structure depends to a great extent on the value of the ground acceleration a_g considered. In order to

study the influence of this parameter, the N2 method proposed by Fajfar and Gaspersic [15] and included in EC-8 [18] is implemented for the structures described in Section 3.1, considering different values for a_g. The structures are built over a C ground type and are located in an area in which the Type 2 spectrum included in EC-8 must be considered. The N2 method is performed for three ground acceleration values (0.1g, 0.2g and 0.3g). The maximum value considered for the ground acceleration (0.3g) is a high enough value for the Type 2 spectrum.

The plastic hinges considered in the different analyses are those described in Section 1. For the different ground acceleration values, the shear force F_b, the spectral acceleration S_a and the distribution of plastic hinges in the structure are obtained. Additional nonlinear time-history analyses are performed for the maximum value of the ground acceleration considered, in order to contrast the results achieved from the pushover analyses.

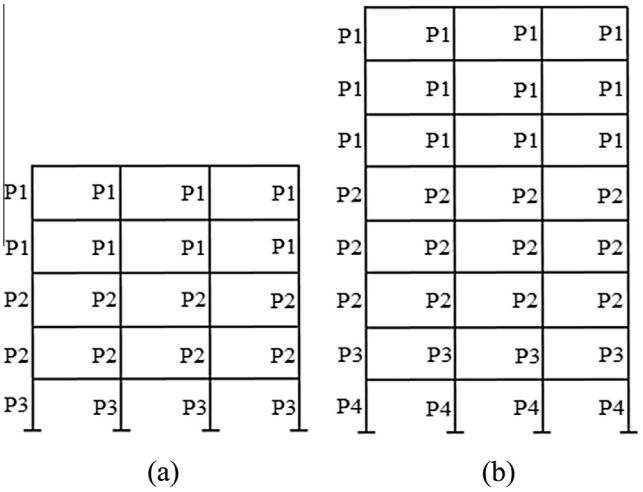

Fig. 5. Elevation view of the analysed structures. (a) 5-storey frame. (b) 8-storey frame.

3. Behaviour of reinforced concrete sections in the structures used as examples

3.1. Description of structures

Two particular cases of structures are studied following the above description of the general considerations related to the sectional behaviour of RC elements and the specific considerations corresponding to pushover analysis. A floor plan of usual 5- and 8-storey RC buildings in Europe is shown in Fig. 4. The layout of these structures is considered as typical of low and medium rise residential buildings of reinforced concrete designed under Eurocode 8 [22]. The elevation view of the structures considered for the pushover analysis is shown in Fig. 5. These structures correspond to the interior frame shown in Fig. 4. The floor-to-floor height is 3 m and the span length is 5 m for both structures. It should be mentioned that these simplified structures have been considered in order to ease the interpretation of the results achieved in the nonlinear analyses and to focus on the differences observed by using the different models of plastic hinges described in Section 1.

The geometry and reinforcement for the cross-sections of the frames are shown in Fig. 6. The frames are composed by beams with the same depth as the floor slabs, and columns with a square section. Material properties are 25 MPa for the concrete compressive strength and 500 MPa for the yield strength of both longitudinal and transverse reinforcement. The hoop spacing is 100 mm in the potential plastic hinge regions. The elastic modulus of the concrete is 27,200 MPa and its Poisson's ratio is 0.2. It should be mentioned that no shear plastic hinges are considered for nonlinear analyses since, as stated in [21], the concrete compressive strength and the spacing of hoops considered in this work are sufficient to prevent shear failures.

Following the aforementioned strategy of considering simplified structures, all the beams have the same dimensions and the reinforcement is constant throughout the beam, even though this means that these structures are not entirely realistic. In the case of wide beams, they have been considered, despite their

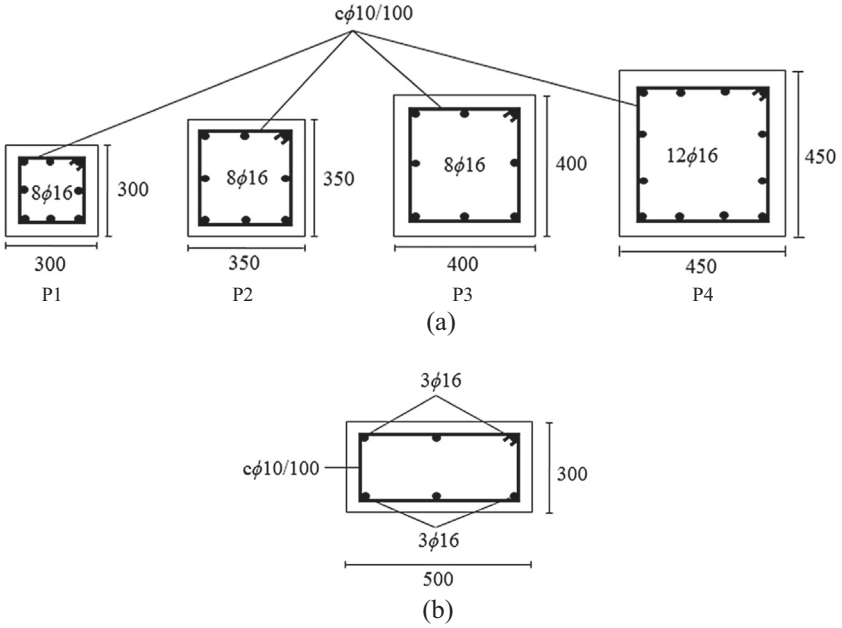

Fig. 6. Cross-sections for elements in 5- and 8-storey frames. (a) Columns. (b) Beams. [Dimensions in mm].

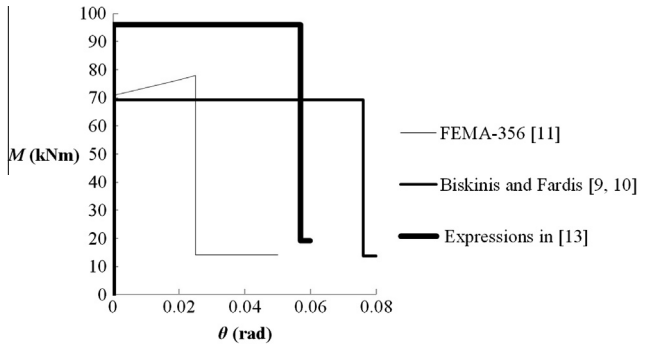

Fig. 7. Moment-chord rotation relation for the RC plastic hinges generated in the beams.

inadequate seismic behaviour, because of their widespread use in countries of the moderate-seismicity Mediterranean area, such as Spain, Italy and Portugal [23].

Concerning gravity loads, dead and live loads are 5 and 3 kN/m^2 respectively, corresponding to residential buildings according to EC-2 [17]. The loads are uniformly distributed on beams. The period T of the fundamental mode that has been obtained is 1.24 s for the 5-storey frame and 1.9 s for the 8-storey frame. These values are obtained assuming lumped masses at storey levels.

3.2. Moment-chord rotation relations and yielding curves

The moment-chord rotation relations obtained with the different methods for the beams and columns are shown in Figs. 7 and 8. For all cases, the expressions proposed in [13] offer higher values of M_y than those obtained by applying the expressions of Biskinis and Fardis [9] and the values obtained with FEMA-356 [11]. The moment-chord rotation relations defined with the expressions developed in [13] show a deformation capacity between those obtained with the other two methods.

Unlike in other studies [21], several yielding curves N-M_y have been defined in this work in order to consider the influence of the axial force N on the yield moment M_y of columns in the nonlinear analyses.

The yielding curves for the columns obtained from the different methods are shown in Fig. 9. The curves obtained from the empirical expressions developed in [9,13] show higher values for M_y than those obtained from FEMA-356 [11]. The maximum values for M_y correspond to the expression proposed in [13]. However, it should be noted that the curves obtained with the expression of Biskinis and Fardis [9] exhibit higher values of M_y for a range of values of the axial force N.

4. Results and discussion

The capacity curves F_b - δ obtained for the frames using plastic hinges defined with the different methods for the uniform and modal lateral load patterns are shown in Fig. 10 and 11. The modal lateral load pattern given by Eq. (13) is adopted for the 8-storey frame in order to consider the effect of higher modes. The plastic hinges modelled with the expressions included in [9,10,13] obtain higher values of F_b than the plastic hinges included by default in SAP2000®. For all cases, the plastic hinges of FEMA-356 [11] and those modelled with the expressions of Biskinis and Fardis [9,10] offer similar values of the seismic base shear force F_b for values of the control displacement δ included in the range (0, 250).

It is important to emphasize the relation between F_b and the yield moment M_y of plastic hinges: as the values of M_y increase, so do those of F_b. This aspect explains the fact that the maximum values of F_b are reached when the plastic hinges modelled with the expressions developed in [13] are considered, since these

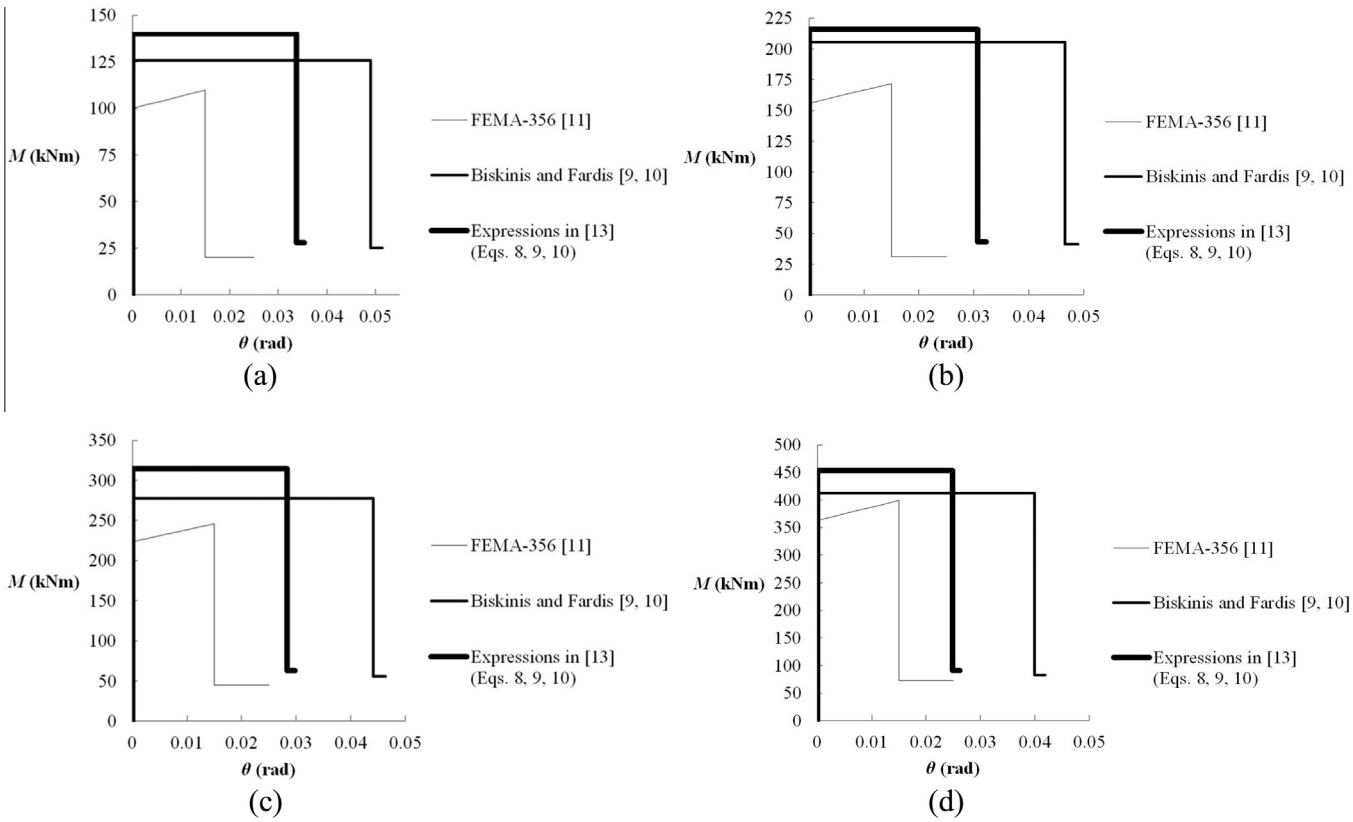

Fig. 8. Moment-chord rotation relations for the RC plastic hinges generated in the columns. (a) P1. (b) P2. (c) P3. (d) P4.

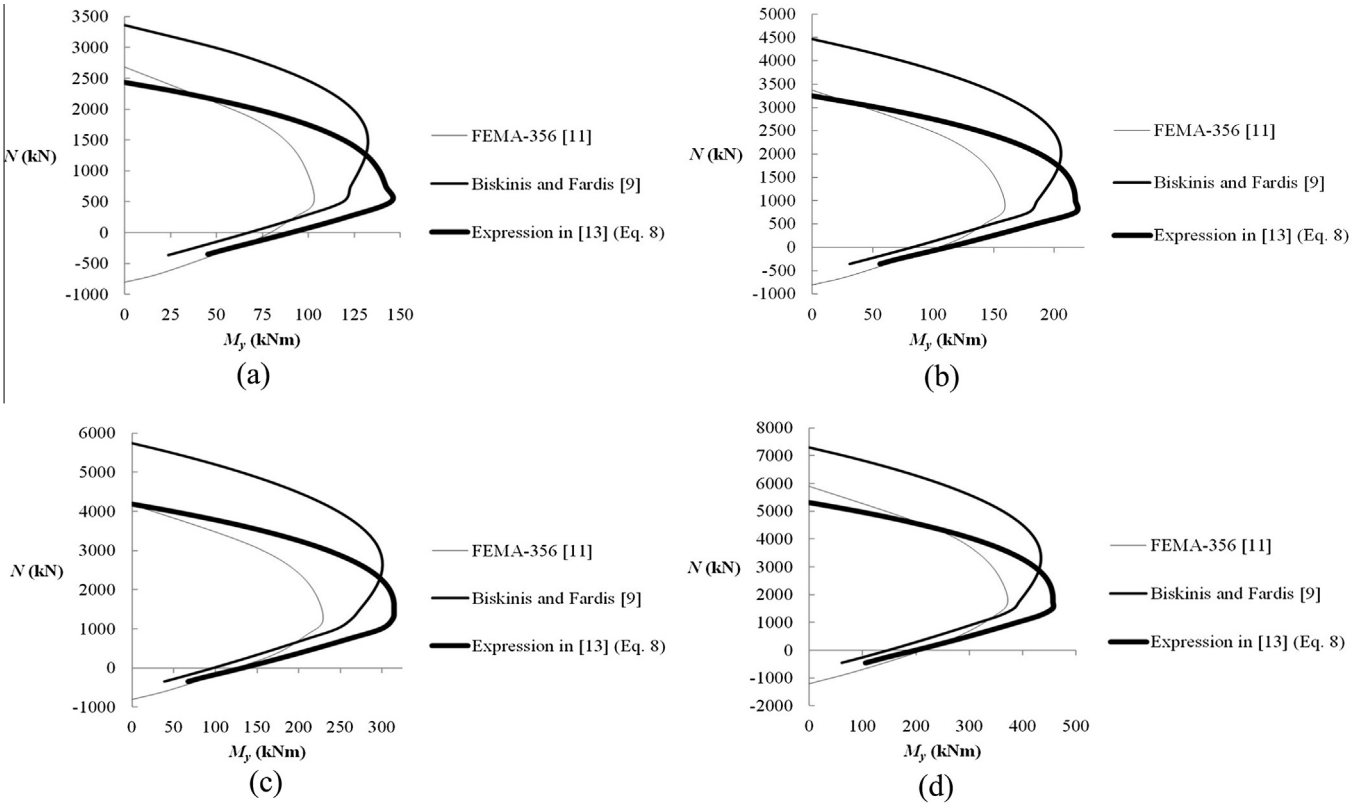

Fig. 9. Yielding curves for columns. (a) P1. (b) P2. (c) P3. (d) P4.

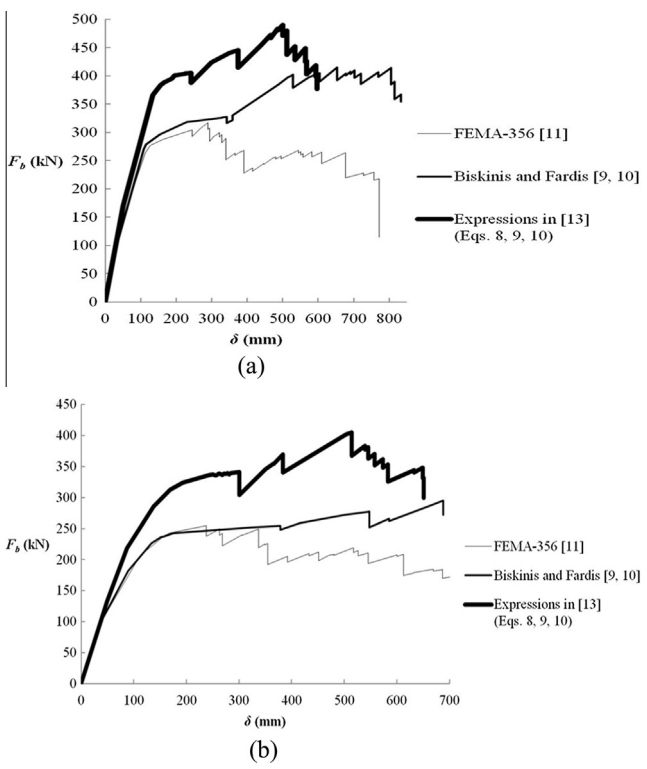

Fig. 10. Capacity curves for the 5-storey frame. (a) Uniform lateral load. (b) Modal lateral load.

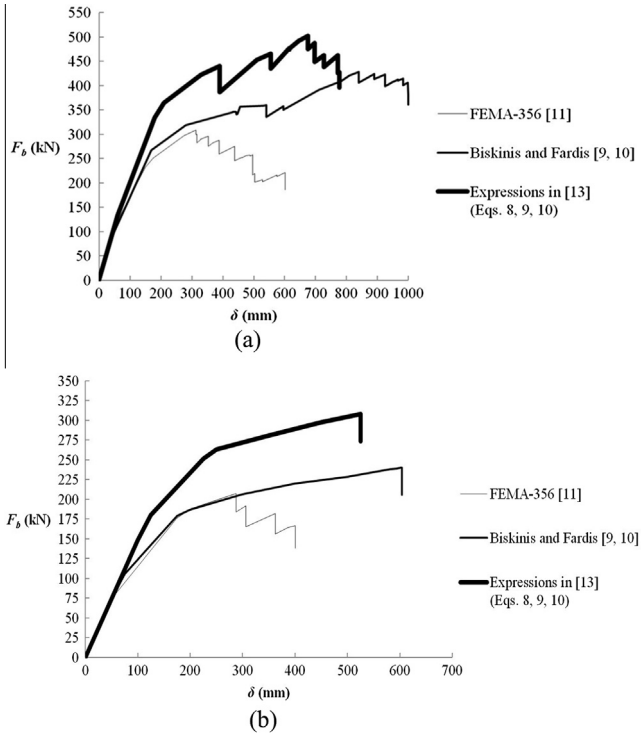

Fig. 11. Capacity curves for the 8-storey frame. (a) Uniform lateral load. (b) Modal lateral load.

plastic hinges offer the maximum values for M_y. Another relevant aspect is the fact that the capacity curves obtained with the expressions proposed in [13] and the expressions of Biskinis and Fardis [9,10] can meet at a certain value of δ, since according to Fig. 9, these expressions can offer the same value for M_y and, consequently, for F_b.

Table 2
Results for the global yielding point of the 5-storey frame.

Plastic hinge	Uniform lateral load			Modal lateral load		
	δ (mm)	F_b (kN)	S_a/g	δ (mm)	F_b (kN)	S_a/g
FEMA-356 [11]	128	278	0.197	169	243	0.189
Biskinis and Fardis [9,10]	116	279	0.204	176	243	0.186
Expressions in [13]	138	370	0.282	194	324	0.250

Table 3
Results for the global yielding point of the 8-storey frame.

Plastic hinge	Uniform lateral load			Modal lateral load		
	δ (mm)	F_b (kN)	S_a/g	δ (mm)	F_b (kN)	S_a/g
FEMA-356 [11]	175	251	0.109	175	176	0.088
Biskinis and Fardis [9,10]	169	267	0.118	175	179	0.089
Expressions in [13]	210	364	0.172	250	263	0.132

Table 4
Results for the collapse point of the 5-storey frame.

Plastic hinge	Uniform lateral load				Modal lateral load			
	δ (mm)	F_b (kN)	S_a/g	Decrease in F_b for the collapse point (%)	δ (mm)	F_b (kN)	S_a/g	Decrease in F_b for the collapse point (%)
FEMA-356 [11]	391	269	0.217	15	354	226	0.153	15
Biskinis and Fardis [9,10]	805	414	0.308	15	547	277	0.212	10
Expressions in [13]	565	449	0.345	16	649	348	0.299	15

Table 5
Results for the collapse point of the 8-storey frame.

Plastic hinge	Uniform lateral load				Modal lateral load			
	δ (mm)	F_b (kN)	S_a/g	Decrease in F_b for the collapse point (%)	δ (mm)	F_b (kN)	S_a/g	Decrease in F_b for the collapse point (%)
FEMA-356 [11]	496	258	0.125	22	400	167	0.088	16
Biskinis and Fardis [9,10]	998	405	0.216	13	604	240	0.126	15
Expressions in [13]	773	462	0.242	15	525	308	0.159	11

Some authors define the global yielding point of a structure as the point of the capacity curve in which the structure ends its linear elastic behaviour [21]. Tables 2 and 3 show the values obtained for the control displacement δ, the seismic base shear force F_b and the spectral acceleration S_a for the global yielding point of the structures. To obtain the value of S_a, it is necessary to transform the capacity curve F_b – δ into the capacity spectrum in the acceleration-displacement format S_a – S_d, applying the equations proposed in [24].

The plastic hinges modelled with the expressions proposed in [13] provide the maximum values of F_b, δ and S_a for all cases, since these expressions offer the maximum values of M_y. The differences with respect to the other methods are between 7 and 42% for δ, and 33 and 49% for F_b, while a maximum difference of 58% is obtained for S_a. The differences between the results obtained with the expressions in [13] and the other methods become greater as the height of the structure increases and if the modal lateral load pattern is considered.

The structural collapse point is also considered, which depends on the safety level that has been adopted. Several authors consider that a structure collapses when a 20% decrease in F_b in the capacity curve is reached [21]. Other authors relate this point to the cross-sectional failure, considering it is reached when a 15% decrease occurs in the lateral load applied in the corresponding experimental test [8]. In this study, a 15% decrease in F_b in the capacity curve is adopted for the structural collapse.

The results obtained for the collapse point of the frames are shown in Tables 4 and 5. If the influence of the height of the structure is studied, the higher flexibility of the 8-storey frame normally entails higher values for δ and lower values for F_b and S_a/g. The expressions of Biskinis and Fardis [9,10] generally provide the highest values for δ, due to the fact that these expressions offer the maximum deformation capacity (Figs. 7 and 8). Moreover, these expressions provide the lowest percentages of decrease in F_b for the collapse point, having considered values below 15% as an exception. The expressions proposed in [13] yield the highest values for F_b, obtaining maximum differences of 84% with respect to the other methods. Regarding S_a, these expressions provide higher values than the other methods, with a maximum difference of 95%.

Tables 6 and 7 show the results obtained for the different values of the ground acceleration a_g. According to EC-8 [18], the target displacement d_t of a structure is defined as the seismic demand derived from the elastic response spectrum in terms of the displacement of an equivalent single-degree-of-freedom system. Since the target displacement is based on a single-degree-of-freedom system behaviour, only the capacity curves obtained with the modal lateral load pattern have been considered in this study. Although the target displacement obtained is the same for the different types of plastic hinges, the differences in the capacity curves (Figs. 10 and 11) provide different values for F_b and S_a if a specific ground acceleration value is considered.

Table 6
Results for the 5-storey frame considering different ground acceleration values.

Ground acceleration a_g/g	Target displacement d_t (mm)	FEMA-356 [11]		Biskinis and Fardis [9,10]		Expressions in [13]	
		F_b (kN)	S_a/g	F_b (kN)	S_a/g	F_b (kN)	S_a/g
0.1	31.3	83	0.078	83	0.080	83	0.082
0.2	62.6	135	0.123	140	0.128	163	0.156
0.3	93.9	180	0.163	186	0.163	226	0.209

Table 7
Results for the 8-storey frame considering different ground acceleration values.

Ground acceleration a_g/g	Target displacement d_t (mm)	FEMA-356 [11]		Biskinis and Fardis [9,10]		Expressions proposed in [13]	
		F_b (kN)	S_a/g	F_b (kN)	S_a/g	F_b (kN)	S_a/g
0.1	35.3	56	0.036	56	0.036	56	0.036
0.2	70.67	91	0.055	100	0.060	105	0.070
0.3	106	120	0.073	129	0.076	156	0.096

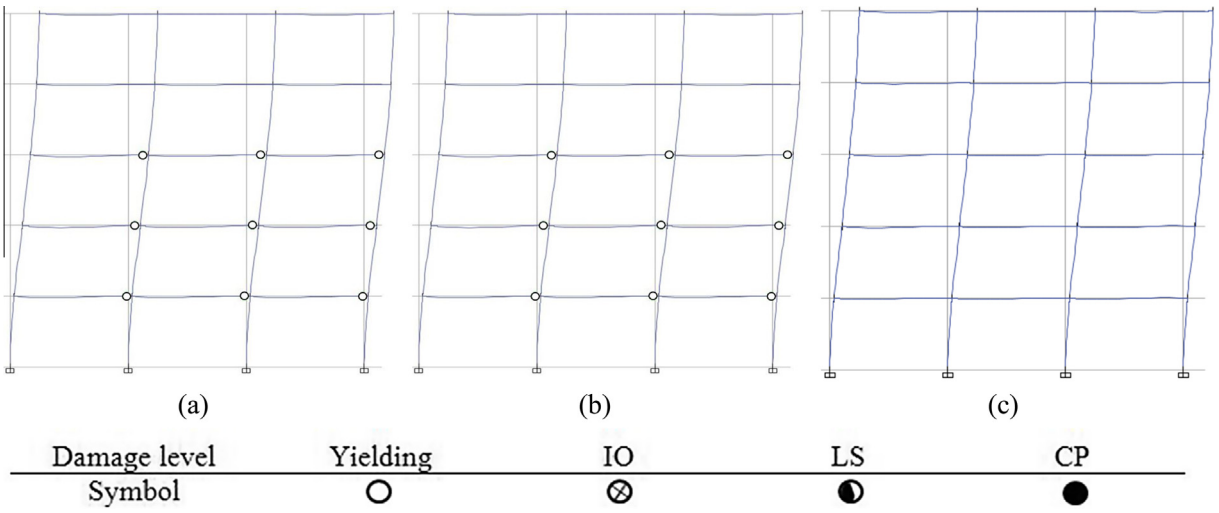

Fig. 12. Plastic hinges distribution for the 5-storey frame and $a_g = 0.2g$. (a) FEMA-356 [11]. (b) Biskinis and Fardis [9,10]. (c) Expressions in [13].

It is important to mention that the differences between the methods are obtained for ground acceleration values higher than $a_g = 0.1g$. These differences increase with the value of the ground acceleration, whereas the height of the structure does not have a significant influence on the results. The values obtained for F_b and S_a are higher if the plastic hinges modelled with the expressions developed in [13] are considered, with the differences being between 14 and 30% for F_b and 5 and 31% for S_a with respect to FEMA-356 [11].

The distribution of the plastic hinges generated in the structure for the different values of the ground acceleration is shown in Figs. 12–15. The results offered correspond to $a_g = 0.2g$ and $a_g = 0.3g$, since, according to Tables 6 and 7, there is no difference in the results obtained with the different types of plastic hinges for $a_g = 0.1g$.

For all cases, the state of the plastic hinges generated corresponds to a point located between the points B and C shown in Figs. 1 and 2. Therefore, the resistance of none of the plastic hinges has fallen for the ground acceleration values considered. The target displacement obtained by considering Type 2 spectrum and low ground acceleration values generates low damage levels. Only the IO structural performance level is achieved for the 5-storey frame considering the plastic hinges modelled with FEMA-356 [11] for $a_g = 0.3g$. The number of plastic hinges generated increases with the value of the ground acceleration. Since the expressions included in [13] offer higher values for the yield moment M_y (Figs. 7 and 8), the number of plastic hinges generated is lower if they are modelled with these expressions. For the lowest value of ground acceleration considered ($a_g = 0.2g$), the structure remains elastic if the plastic hinges modelled with the expressions in [13] are considered.

In order to show the capability of the different methods for detecting plastic hinges for the columns, the plastic hinges distribution for the displacement of the collapse point obtained from the expressions proposed in [13] is achieved. The displacement obtained with these expressions is considered since it is large enough to induce plastic hinges in columns. The uniform and modal lateral load patterns are considered for 5- and 8-storey frames, respectively. The results obtained with the plastic hinges modelled using the expressions proposed in [13] are only compared with those obtained considering the equations developed by Biskinis and Fardis [9,10], since the displacement imposed is higher than the displacement capacity obtained considering the plastic hinges modelled by FEMA-356 [11].

Figs. 16 and 17 show no significant differences in the plastic hinges distribution for both methods and similar locations for

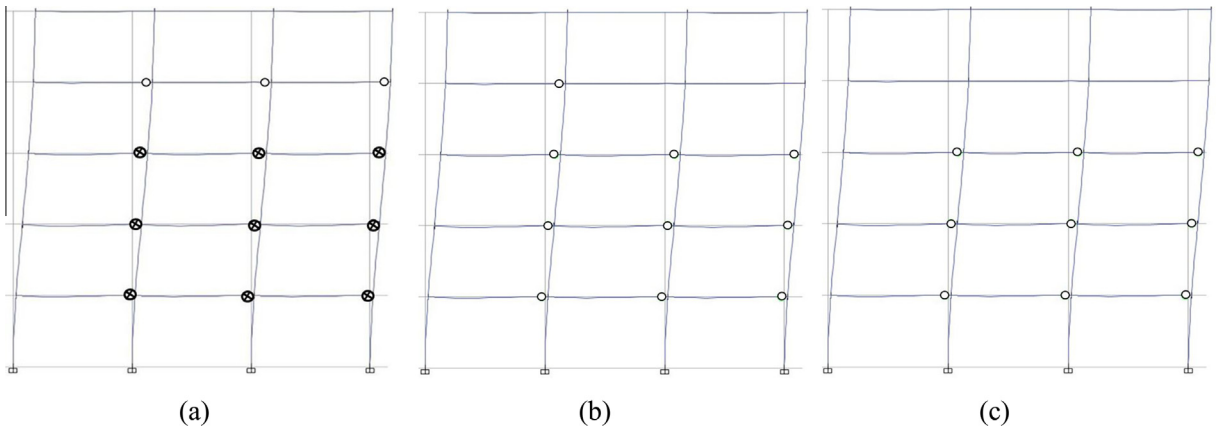

Fig. 13. Plastic hinges distribution for the 5-storey frame and $a_g = 0.3g$. (a) FEMA-356 [11]. (b) Biskinis and Fardis [9,10]. (c) Expressions in [13].

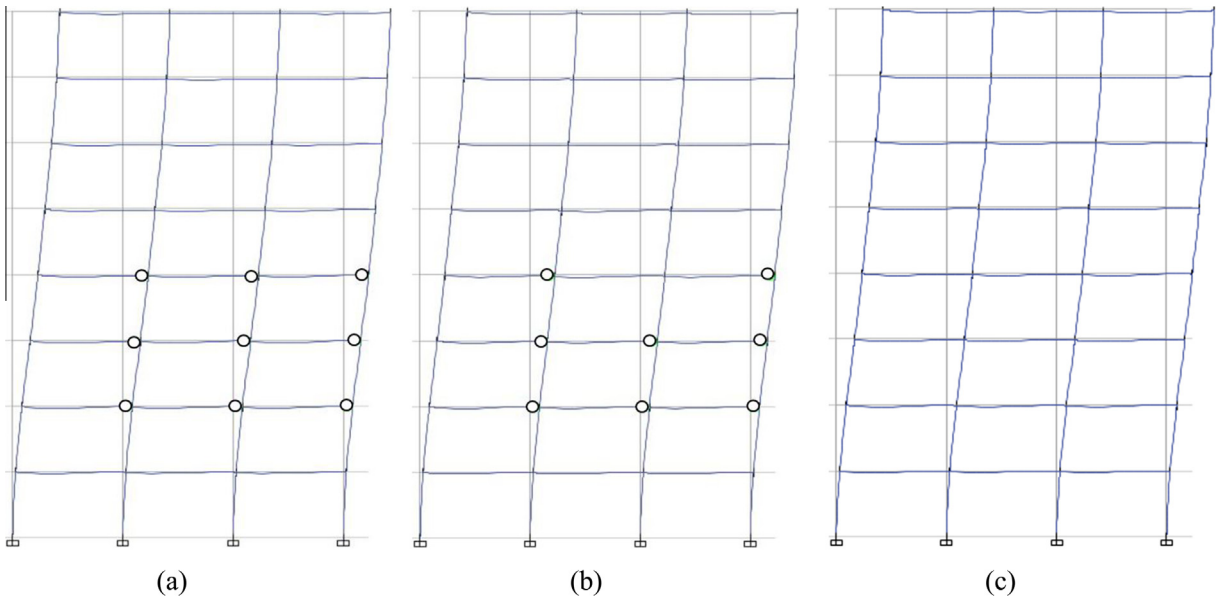

Fig. 14. Plastic hinges distribution for the 8-storey frame and $a_g = 0.2g$. (a) FEMA-356 [11]. (b) Biskinis and Fardis [9,10]. (c) Expressions in [13].

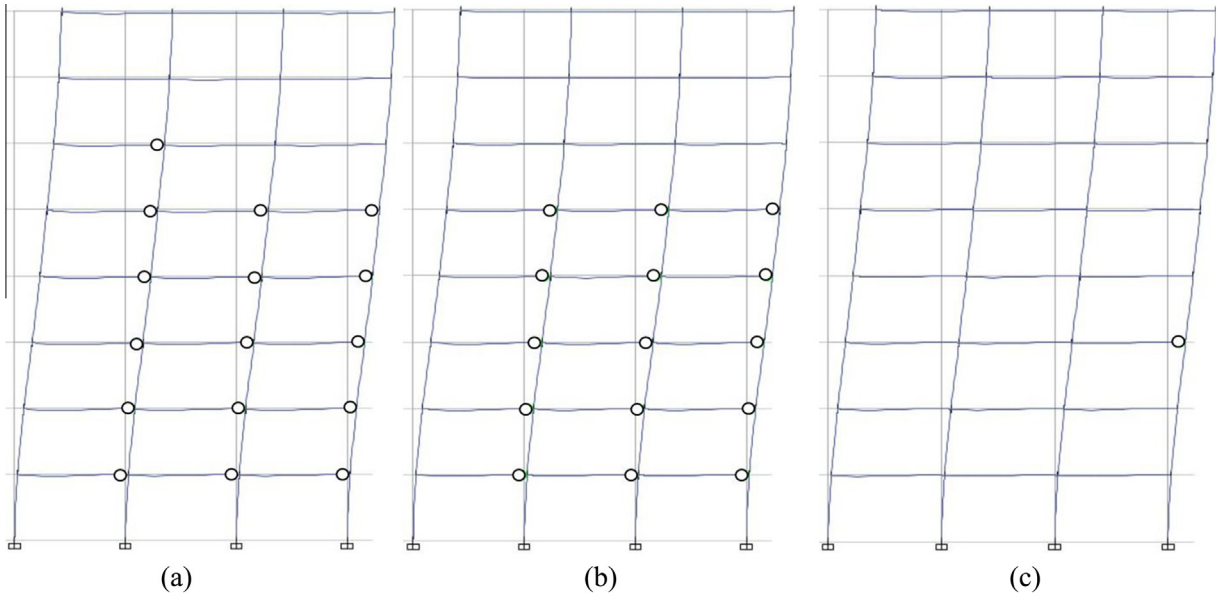

Fig. 15. Plastic hinges distribution for the 8-storey frame and $a_g = 0.3g$. (a) FEMA-356 [11]. (b) Biskinis and Fardis [9,10]. (c) Expressions in [13].

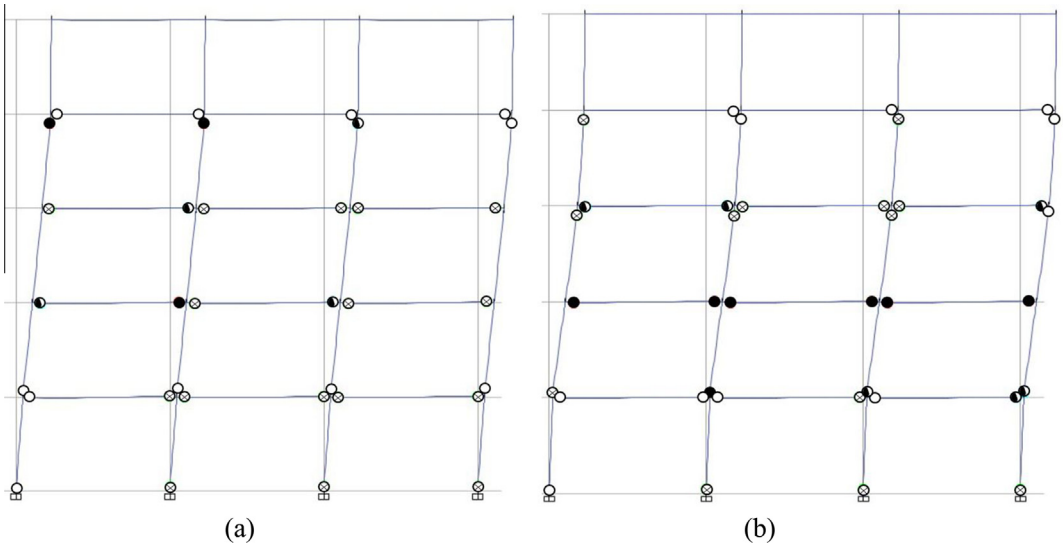

Fig. 16. Plastic hinges distribution for the 5-storey frame in the collapse point. (a) Biskinis and Fardis [9,10]. (b) Expressions proposed in [13].

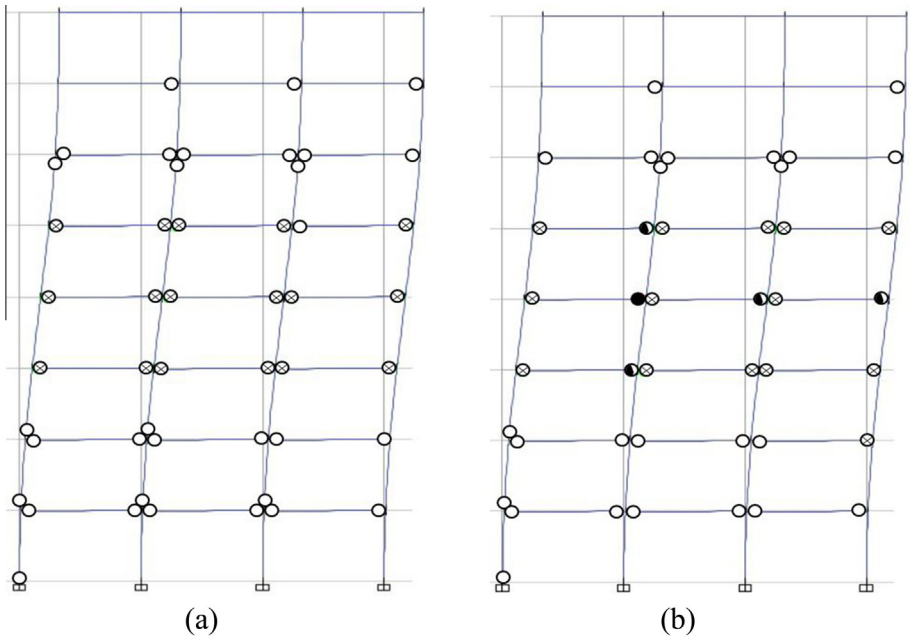

Fig. 17. Plastic hinges distribution for the 8-storey frame in the collapse point. (a) Biskinis and Fardis [9,10]. (b) Expressions proposed in [13].

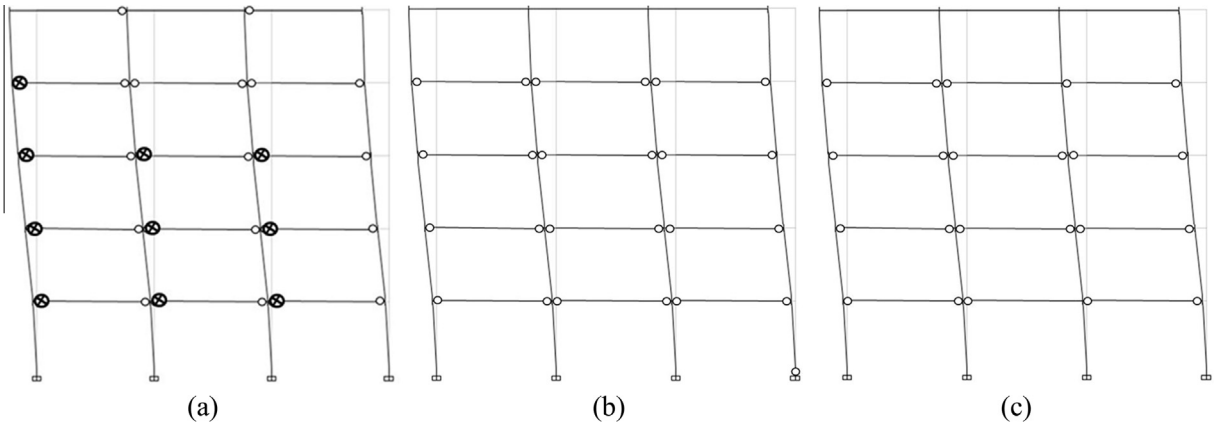

Fig. 18. Time history analysis results for 5-storey frame subjected to El Centro ground motion. (a) FEMA-356 [11]. (b) Biskinis and Fardis [9,10]. (c) Expressions in [13].

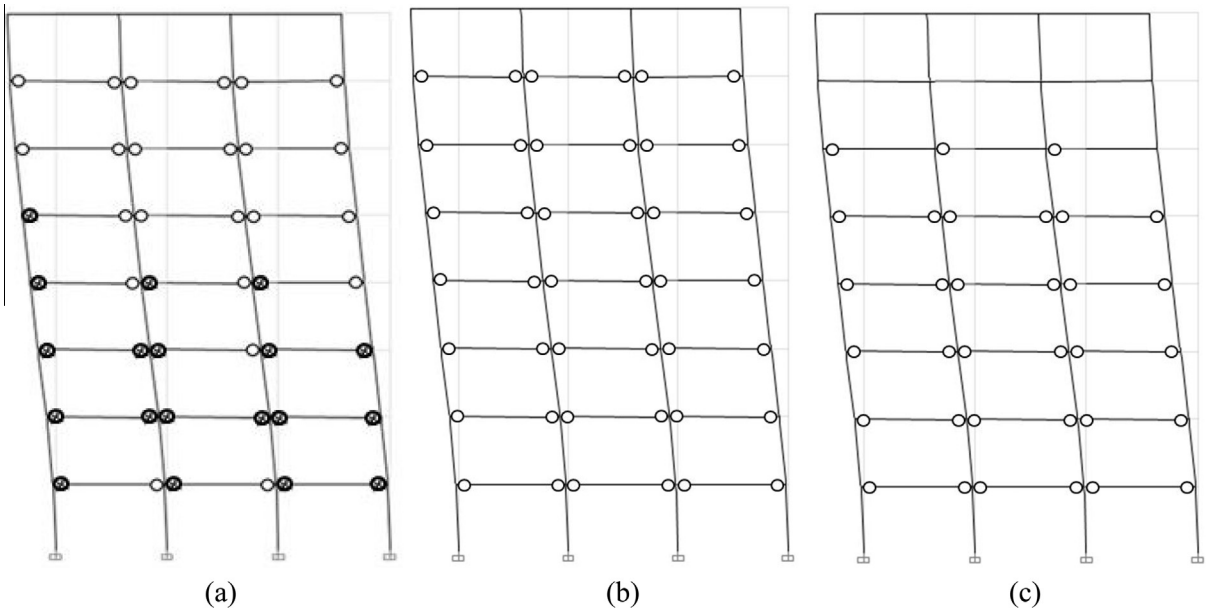

Fig. 19. Time history analysis results for 8-storey frame subjected to El Centro ground motion. (a) FEMA-356 [11]. (b) Biskinis and Fardis [9,10]. (c) Expressions in [13].

the plastic hinges generated in columns. However, the expressions proposed in [13] generally show higher damage levels for both frames, especially in the mid storeys.

It has been considered useful to additionally perform several nonlinear time-history analyses on the 5 and 8-storey structures, using different accelerograms, in order to compare the structural response to that achieved with pushover analyses. Each earthquake has its own characteristics (frequency content, duration, sequence of peaks and amplitude), and thus provokes a unique response in a certain structure that is different to that resulting from other earthquakes [6,25].

As an example, results from the nonlinear time-history analysis using the accelerogram of the El Centro earthquake (records taken every 0.01 s and 40 s of total duration) are shown. Geometric configurations and distributions of plastic hinges obtained when the maximum displacement of the top storey is achieved are included in Figs. 18 and 19. The similarity between the results obtained from the pushover analysis with modal lateral loads and adopting $a_g = 0.3g$ (Figs. 13 and 15), and those obtained from the nonlinear time-history analysis can be observed. Although more plastic hinges are developed in the structure when implementing nonlinear time-history analyses, only the plastic hinges modelled with FEMA-356 [11] achieve the IO structural performance level. Moreover, a lower number of plastic hinges are developed in the structure when considering the expressions proposed in [13].

5. Conclusions

The influence of the type of plastic hinge considered in the nonlinear behaviour of RC planar frames has been evaluated in this paper. Several nonlinear analyses have been performed considering plastic hinges modelled with different methods, including some empirical equations for the sectional behaviour, which obtain parameters related to the yielding and ultimate states. Since the main aim of this work is the comparison between methods, simplified analyses and structures are considered in order to clarify the contrast in the results.

The higher resistance and deformation capacity of a section offered by the expressions proposed in [13] with respect to the other methods justifies the obtaining of higher values for the seismic base shear force F_b and the control displacement δ, which implies a higher resistance and deformation capacity from the structural point of view. Furthermore, a more favourable plastic hinges distribution is obtained for the structure. However, the higher values obtained for the spectral acceleration S_a are indicative of higher forces in the structure when the seismic load acts.

These aspects enable the structural engineer to check whether the plastic hinges included in structural codes offer too conservative results. The comparison between the different methods to model the plastic hinges is more interesting with the increase of the height of the structure and the ground acceleration and if the modal lateral load pattern is considered in the analysis.

Since the expressions developed in [13] are calibrated with a selection of tests that meet the seismic and construction requirements imposed by the main international design codes, the plastic hinges calibrated with the aforementioned expressions are suitable for a wider range of cases than the plastic hinges included by default in structural codes, which are usually defined with values corresponding to RC elements used in those countries where one specific design code is applied.

On the other hand, the fact of being calibrated with a less heterogeneous database of experimental tests reduces the scatter offered by the expressions proposed in [13] with respect to the expressions proposed by Biskinis and Fardis [9,10]. Therefore, the expressions developed in [13] are more suitable for simulating the sectional behaviour that is required to model the plastic hinges developed in the nonlinear analysis of ordinary RC buildings.

References

[1] Chopra AK, Goel RK. A modal pushover analysis procedure for estimating seismic demands for buildings. Earthq Eng Struct Dyn 2002;31(3):561–82. http://dx.doi.org/10.1002/eqe.144.
[2] Poursha M, Khoshnoudian F, Moghadam AS. A consecutive modal pushover procedure for estimating the seismic demands of tall buildings. Eng Struct 2009;31(2):591–9. http://dx.doi.org/10.1016/j.engstruct.2008.10.009.
[3] Jan TS, Liu MW, Kao YC. An upper-bound pushover analysis procedure for estimating the seismic demands of high-rise buildings. Eng Struct 2004;26(1):117–28. http://dx.doi.org/10.1016/j.engstruct.2003.09.003.
[4] Kim SP, Kurama YC. An alternative pushover analysis procedure to estimate seismic displacement demands. Eng Struct 2008;30(12):3793–807. http://dx.doi.org/10.1016/j.engstruct.2008.07.008.
[5] Aydinoglu MN. An incremental response spectrum analysis procedure based on inelastic spectral displacements for multi-mode seismic performance

evaluation. Bull Earthq Eng 2003;1(1):3–36. http://dx.doi.org/10.1023/A:1024853326383.
[6] Fardis MN. Seismic design, assessment and retrofitting of concrete buildings based on EN-Eurocode 8. Netherlands: Springer; 2009.
[7] Taghavipour S, Majid TA, Liang LT. Effect of different lateral load distribution on pushover analysis. Aust J Basic Appl Sci 2013;7(4):133–42.
[8] Panagiotakos TB, Fardis MN. Deformations of reinforced concrete members at yielding and ultimate. ACI Struct J 2001;98(2):135–48. http://dx.doi.org/10.14359/10181.
[9] Biskinis D, Fardis MN. Deformations at flexural yielding of members with continuous or lap-spliced bars. Struct Concr 2010;11(3):127–38.
[10] Biskinis D, Fardis MN. Flexure-controlled ultimate deformations of members with continuous or lap-spliced bars. Struct Concr 2010;11(2):93–108. http://dx.doi.org/10.1680/stco.2010.11.2.93.
[11] Federal Emergency Management Agency. Prestandard and commentary for the seismic rehabilitation of buildings. FEMA-356. Washington, D. C.: FEMA; 2000.
[12] SAP2000 v16 Academic. Berkeley: Computers & Structures, Inc.; 2013.
[13] López-López A, Tomás A, Sánchez-Olivares G. Behaviour of reinforced concrete rectangular sections based on tests complying with seismic construction requirements. Struct Concr 2016. http://dx.doi.org/10.1002/suco.201500107 [in press].
[14] López-López AT. Behaviour models of reinforced concrete sections adjusted with experimental tests using metaheuristics algorithms. PhD thesis; 2015 [in Spanish].
[15] Fajfar P, Gaspersic P. The N2 method for the seismic damage analysis of RC buildings. Earthq Eng Struct Dyn 1996;25(1):31–46. http://dx.doi.org/10.1002/(SICI)1096-9845(199601)25:1<31::AID-EQE534>3.0.CO;2-V.
[16] EN 1998-3. Eurocode 8, design of structures for earthquake resistance. Part 3: assessment and retrofitting of buildings.. Brussels: Commission of the European Communities; 2005.
[17] EN 1992-1-1. Eurocode 2, design of concrete structures. Part 1.2: general rules and rules for buildings. Brussels: Commission of the European Communities; 2004.
[18] EN 1998-1. Eurocode 8, design of structures for earthquake resistance. Part 1.3: general rules-specific rules for various materials and elements. Brussels: Commission of the European Communities; 2005.
[19] ACI Committee 318. Building code requirements for structural concrete (ACI 318-08) and commentary (318R-08). Farmington Hills: American Concrete Institute; 2008.
[20] Mortezaei A, Ronagh HR. Effectiveness of modified pushover analysis procedure for the estimation of seismic demands of buildings subjected to near-fault ground motions having fling step. Nat Hazards Earth Syst 2013;13:1579–93. http://dx.doi.org/10.5194/nhess-13-1579-2013.
[21] Inel M, Ozmen HB. Effects of plastic hinge properties in nonlinear analysis of reinforced concrete buildings. Eng Struct 2006;28(11):1494–502. http://dx.doi.org/10.1016/j.engstruct.2006.01.017.
[22] Carvalho EC, Coelho E, Fardis MN. Assessment of EC8 provisions for reinforced concrete frames. In: 11th world conf on earthquake engineering. paper 2049.
[23] Benavent-Climent A. Influence of hysteretic dampers on the seismic response of reinforced concrete wide beam–column connections. Eng Struct 2006;28:580–92. http://dx.doi.org/10.1016/j.engstruct.2005.09.013.
[24] Applied Technology Council. Seismic evaluation and retrofit of concrete buildings. ATC-40. California: Applied Technology Council; 1996.
[25] Mwafy AM, Elnashai AS. Static pushover versus dynamic collapse analysis of RC buildings. Eng Struct 2001;23:407–24.